Organic Semiconductors: Polymorphism, Phonon Dynamics and Carrier-Phonon Coupling in Pentacene

R. G. Della Valle [a] , A. Brillante [a] , L. Farina [a] , E. Venuti [a] , M. Masino [b] & A. Girlando [b]

[a] Dip. Chimica Fisica ed Inorganica and INSTM-UdR Bologna, Bologna Univ., Bologna, Italy

[b] Dip. Chimica G.I.A.F. and INSTM-UdR Parma, Parma University, Parma, Italy

Version of record first published: 18 Oct 2010

PLEASE SCROLL DOWN FOR ARTICLE

Taylor & Francis
Taylor & Francis Group

ORGANIC SEMICONDUCTORS: POLYMORPHISM, PHONON DYNAMICS AND CARRIER-PHONON COUPLING IN PENTACENE

R. G. Della Valle, A. Brillante, L. Farina, and E. Venuti
Dip. Chimica Fisica ed Inorganica and INSTM-UdR Bologna,
Bologna Univ. I-40136 Bologna, Italy

M. Masino, and A. Girlando
Dip. Chimica G.I.A.F. and INSTM-UdR Parma, Parma University,
I-43100 Parma, Italy

The crystal structure and phonon dynamics of pentacene is computed with the Quasi Harmonic Lattice Dynamics (QHLD) method, based on atom-atom potential. We show that two crystalline phases of pentacene exist, rather similar in thermodynamic stability and in molecular density. The two phases can be easily distinguished by Raman spectroscopy in the 10–100 cm^{-1} spectral region. We have not found any temperature induced phase transition, whereas a sluggish phase change to the denser phase is induced by pressure. The bandwidths of the two phases are slightly different. The charge carrier coupling to low-frequency phonons is calculated.

INTRODUCTION

Despite recent progresses [1], the development of electronic devices based on organic semiconductors remains an open challenge. Considerable attention has been recently devoted to pentacene, due to the claim of mobilities comparable to crystalline silicon, and other extraordinary properties [2]. Such claims have been show to be invalidated by scientific misconduct [3], yet pentacene still holds the record of highest room temperature mobility among materials for organic thin-film transistors. This record

R. G. Della Valle et al.

mobility of about $1.5\,cm^2V^{-1}s^{-1}$ has been reached by continuous improvements in the sample chemical purification [1]. On the other hand, the crystal and thin film growth also have paramount importance for device performance, together with a proper understanding of the motion of charge carriers inside the crystal. By combining computational and experimental approaches, we have addressed the above problems for the specific case of pentacene. Here we review the main results reached so far.

CRYSTAL STRUCTURES

The polymorphism of pentacene, both in bulk and in thin film, has been object of intense experimental [4–6] and theoretical [7,8] studies. We have analyzed the five complete X-ray structures of pentacene single crystal crystal reported so far by computing the "inherent structures", defined as the local minima of the potential energy hypersurface [9]. Each structure was modeled starting from its experimental molecular arrangements and a common *ab-initio* molecular geometry. The identity of molecular geometries in all the configurations is a necessary prerequisite for allowing identical phases to map into identical potential minima. The theoretical structures of mechanical equilibrium were determined by minimizing the potential energy, Φ. The unit cell axes, angles, molecular orientations and positions were freely varied in the minimization. At this stage, we adopted the rigid molecule approximation, retaining the molecular geometry fixed. The intermolecular potential was represented by an atom-atom Buckingam model, with Williams parameters set IV, plus electrostatic interactions described by the *ab-initio* charges residing on the atoms [9].

With the above described method, we have been able to show that the five reported crystal structures correspond to two different "inherent structures", i.e., two local Φ minima. One of the minima, labeled as phase **C**, corresponds to the structure determined by Campbell *et al.* [4]. The other polymorph, phase **H**, corresponds to the structure found in the more recent measurements [5]. Both polymorphs belong to the triclinic system, space group $P\overline{1}$ (C_i) with two molecules per unit cell arranged in the usual herringbone pattern. Figure 1 compares the two structures, which appear to be very similar, the main difference being a shift of the two molecules along the long molecular axis, yielding different $d(001)$-spacings (14.5 *vs* 14.1 Å for **C** and **H** phases [6]).

We have extended the analysis by systematically sampling the potential hypersurface to gain information on the *global* stability of the minima. In the case of pentacene, a quasi-Monte Carlo search yielded several hundred of distinct minima, with surprising variety of structural arrangements [10].
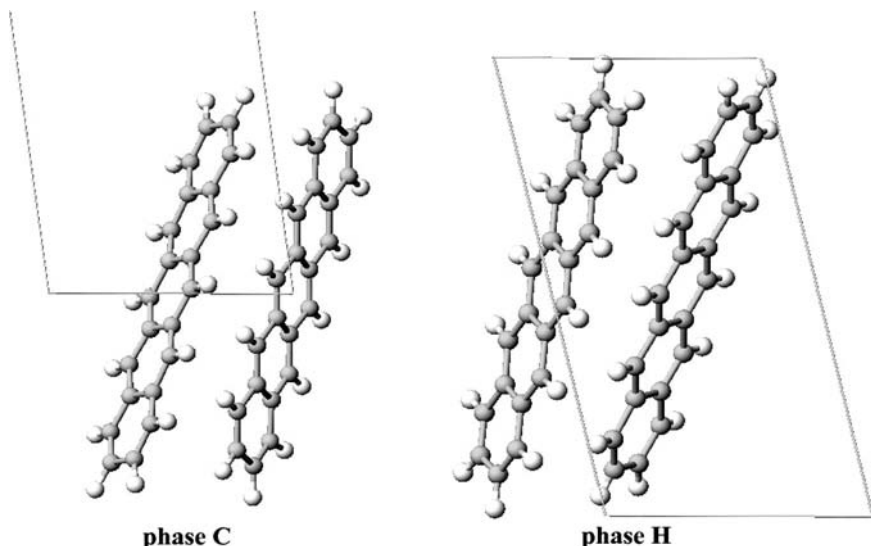
FIGURE 1 Comparison of pentacene **C** and **H** polymorphs.

On the other hand, deep minima are easily accessible since their attraction basin tends to be wide. We found that the two deepest minima indeed correspond to the experimental **C** and **H** polymorphs, which are described correctly. Other deep minima with layered structures, which might correspond to the thin film polymorphs found to grow on substrates, were also found.

After the above analysis of the potential energy Φ, we have accounted for the effects of temperature T and pressure p by calculating the structures of minimum Gibbs energy $G(p,T)$ with the quasi harmonic lattice dynamics (QHLD) methods [9]. In this method the vibrational contribution to the Gibbs energy is estimated in the harmonic approximation:

$$G(p,T) = \Phi + pV + \sum_{\mathbf{q},j} \frac{\hbar\omega_{\mathbf{q},j}}{2} + k_{\mathrm{B}}T \sum_{\mathbf{q},j} \ln\left[1 - \exp\left(-\frac{\hbar\omega_{\mathbf{q},j}}{k_B T}\right)\right] \quad (1)$$

Here V is the molar volume, and $\omega_{\mathbf{q},j}$ are the harmonic phonon frequencies, calculated by diagonalizing the dynamical matrix obtained from the second derivatives of Φ with respect to the displacements of the jth molecular coordinate with wavevector $\mathbf{q}$. The second term in Eq. (1) is the zero-point energy, and the last term is the entropic contribution. The sums are extended to all phonon frequencies. Since pentacene exhibits *ab-initio* intra-molecular frequencies as low as $38\,\mathrm{cm}^{-1}$, we had to allow for the coupling between lattice and intra-molecular vibrations, found to be necessary in similar cases. We adopted an exciton-like model [11], where the

interaction between different molecular coordinates is mediated by the intermolecular potential which, being a function of the interatomic distance, depends directly on the atomic displacements. Since these correspond to the cartesian eigenvectors of the normal modes of the isolated molecule, we used the *ab-initio* eigenvectors and the scaled *ab-initio* frequencies. Intra-molecular modes above $300\,cm^{-1}$ were not taken into account, because coupling is important only for low frequency modes.

Comparison between minimum Φ and minimum G structures shows that the latter, which include vibrational effects, brings the calculated volumes from about 4% to about 2% from experimental values, or better. Moreover, the minimum G calculations reproduce correctly the thermal expansion of the **H** phase. The experimental volume expansion from 90 to 293 K is 3.5%, to be compared with a calculated value of 2.7%. The coupling between lattice and intra-molecular vibrations is important, since the calculated expansion falls down to 1.9% by neglecting it [9].

For both phases, the QHLD calculations exhibit a mechanical instability at $T > 550\,K$, where no minimum of $G(p,T)$ can be found and the crystal structure diverges. Experimental melting temperatures are given between 540 and 580 K. As discussed elsewhere [12], loss of mechanical stability in QHLD calculations is not necessarily coincident with melting, but is often close to it. A good agreement is also found for the experimental sublimation heat $\Delta_{sub}H = 184 \pm 10\,kJ/mol$, which is to be compared with the Gibbs energy calculated at 0 K, $G \sim 174\,kJ/mol$ for both phases.

LATTICE PHONON SPECTRA

Although the above QHLD calculations clearly indicate that both **C** and **H** polymorphs are mechanically and thermodynamically stable, one might still harbor doubts about the existence of the form reported by Campbell *et al.* [4], since all the recent X-ray studies have failed to reproduce it. Both the minimum Φ and minimum G calculations indicate that the lowest frequency inter-molecular (lattice) vibrations should differ considerably in **C** and **H** polymorphs. We have then chosen to use Raman scattering in the lattice phonon region ($10–150\,cm^{-1}$). This choice was also supported by the possibility of interfacing optical microscopy to Raman spectroscopy, achieving a spatial resolution of about $1\,\mu m$, which enables a careful mapping of the physical features of each crystal sample. The spectrometer used was a Jobin–Yvon T64000 triple monochromator, interfaced to an Olympus BX40 microscope, and with excitation from a Kripton laser at 752.5 nm. Pentacene crystals (generally metal-like bluish platelets) from different commercial sources were used, without further purification, as samples for the Raman measurements. A different morphology, i.e., tiny blue

microcrystals, was obtained for samples vapor-grown by fast sublimation in Ar or N_2 atmosphere. The Raman spectra were measured by using the above described different crystal samples. The crystals 'physical purity' was checked by mapping their phonon spectra in several spots of the sample.

Figure 2 reports typical Raman profiles in the region $20–250\,\mathrm{cm}^{-1}$, where all the lattice, as well as a number of low-frequency intra-molecular modes, are present. Indeed, as we have already pointed up, some intra-molecular modes occurring in this spectral region are coupled with lattice phonons. A detailed assignment of the spectra is reported elsewhere
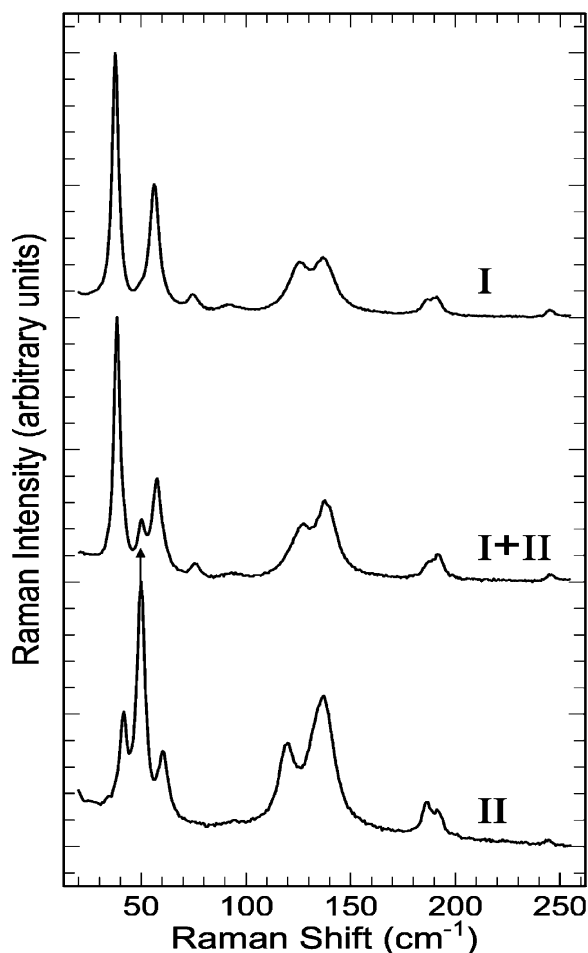

FIGURE 2 Typical Raman spectra of pentacene crystals (from Ref. [13]).

[13,14]. Here, we focus on the lowest frequency bands (below $100\,\mathrm{cm}^{-1}$) which differ significantly in spectrum I and II. In spectrum I, one identifies four bands almost uniformly spread in the considered frequency range. In the case of spectrum II, instead, the three lowest bands are clustered in a narrow frequency range around $55\,\mathrm{cm}^{-1}$, and one very weak band is found near $100\,\mathrm{cm}^{-1}$. This is precisely the frequency pattern we calculated for polymorph **H** and **C**, respectively. Thus commercial samples, which give spectrum I, all belong to the **H** phase, whereas the samples obtained by fast sublimation in inert atmosphere give spectrum II and correspond to phase **C**.

A further remark should be made on Figure 2: the spectra originating from commercial samples (polymorph **H**, morphologically platelets) evidence in some cases an additional feature at $\sim 50\,\mathrm{cm}^{-1}$, as shown by the arrow in the spectrum (I + II) of the same figure. This band is clearly due to a physical residual impurity of polymorph **C** (morphologically microcrystals), that can be monitored in regions of the commercial specimens extended only few microns, as indicated by the decreasing intensity of the band on increasing the crystal area sampled. The fact that a residual presence of polymorph **C** can be found in different amounts on the measured crystals is certainly related to the different degree of physical purity of the used commercial products.

The Raman indications have been subsequently confirmed by direct X-ray measurements [15], which indeed yield two distinct structures, matching the published measurements for forms **C** and **H**. However, the Raman tool is more versatile, and allows one to analyze the phase homogeneity, which, as discussed below, might have important consequences on the measured mobilities. Although identified only in recent years, the phase **H** is the most easily encountered, irrespectively on the method of preparation, either from sublimation or from solution. One therefore expects it is the thermodynamically stable form, even if our calculations indicate a almost equivalent stability for the two phases. We have then decided to investigate the possible presence of phase transitions as a function temperature and of pressure by using the Raman microprobe technique. At the same time, we could verify that the *T, p* evolution of the phonon frequencies is well reproduced by the computed QHLD frequencies [14,15].

No phase transition was detected by changing *T* from 400 to $4.2\,\mathrm{K}$ [14]. On the other hand, we have found that phase **C** starts to irreversibly transform to the denser **H** phase by just applying a moderate pressure of about $0.2\,\mathrm{Gpa}$ [15]. However, the phase transition goes to completion only when pressures up to at least $5\,\mathrm{GPa}$ are applied. Although increasing pressure is obviously expected to favor the higher density **H** phase, the transition mechanism cannot be explained on the basis of relative densities only. In fact, thermal annealing at $p = 0.6\,\mathrm{GPa}$ does not help to speed up the structural change started at $0.2\,\mathrm{GPa}$. Together with the sluggish

evolution of the transition at room temperature, this is an indication that either a high energy barrier must be overcome, or that the driving force becomes weaker under pressure.

CHARGE CARRIER-PHONON COUPLING

Despite intensive research, we still lack of a proper description of the charge carriers motion in organic molecular semiconductors [16]. The problem is a difficult one, since bandwidths, electron-electron interactions, polarization energies, and electron-phonon coupling are all comparable in magnitude. In this paper we shall simply try to estimate the *relative* magnitude of some of the involved parameters.

There is general agreement that the intrinsic mobilities of oligoacenes exhibit a hopping-to-band transition around room temperature [17]. Here, we consider only the bandlike regime, describing the electronic structure in a tight-binding scheme. We have first calculated the intermolecular hopping integrals between pairs of molecules as the splitting of HOMO and LUMO levels from the isolated molecule to the pair by using the INDO/S semi-empirical method [18]. The most important integrals, labeled t_{a1}, t_{a2}, t_{d1}, and t_{d2}, are shown in Figure 3.

The band dispersions are obtained by:

$$\epsilon_\pm(\mathbf{k}) = (t_{a1} + t_{a2})\cos(\mathbf{ka}) \pm 4\{t_{dl}\cos[\mathbf{k(a+b)}/2] + t_{d2}\cos[\mathbf{k(a-b)}/2]\} \tag{2}$$

The resulting bandwidths for **C** and **H** computed structures are reported in Table 1. The temperature dependence is also given. As it usually happens in
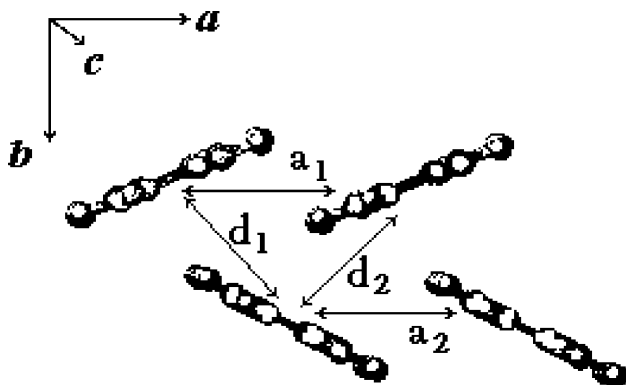

FIGURE 3 Definition of pentacene largest hopping integrals.

R. G. Della Valle et al.

TABLE 1 Calculated VB and CB Bandwidths as a Function of Temperature and Structure

Structure		T = 0 K	150 K	300 K
C	Valence Band (VB)	548 meV	511 meV	470 meV
	Conduction Band (CB)	588 meV	548 meV	508 meV
H	Valence Band (VB)	632 meV	585 meV	536 meV
	Conduction Band (CB)	672 meV	624 meV	576 meV

this kind of calculations [17], the conduction band (CB) is wider than the valence band (VB), contrary to what it would be expected, since in oligo-acenes hole mobility is larger than electron mobility. We believe this is at least in part due to a computational artifact, since in an Hartree-Fock scheme filled orbital are better calculated than virtual orbital energies. So we concentrate on *relative* variations. The lattice contraction by lowering temperature brings about 15% bandwidth increase. More importantly, a similar difference in bandwidth exists between polymorph **C** and **H**, wider bands being of course found in the denser polymorph **H**. Therefore, **C** microdomains embedded in the commonly grown H phase would likely reduce the band mobility, beside the obvious effects of defect scattering at the grain boundaries.

Extensive theoretical and experimental studies have been devoted to the characterization of charge carrier coupling to molecular vibrations, which modulate on-site energies (Holstein coupling) [19]. On the other hand, very little is know about the coupling to inter-molecular, or lattice, phonons (Peierls coupling), despite the fact that lattice phonons are thought to affect mobilities even at low temperatures [16]. In molecular crystals like pentacene, lattice phonons are expected to couple to charge carriers mainly by modulating the amplitude of inter-molecular hopping integrals. The corresponding linear Peierls coupling constants are defined by:

$$g(\mathbf{q}, \mathrm{j}) = \sqrt{\frac{\hbar}{2\omega_{\mathbf{q},\mathrm{j}}}} \left(\frac{\partial t}{\partial Q_{\mathbf{q},\mathrm{j}}}\right)_0 \tag{3}$$

where $Q_{\mathbf{q},\mathrm{j}}$ is the normal coordinate for the jth phonon with wavevector $\mathbf{q}$. We have assumed the low-frequency phonons, mainly inter-molecular in character, as dispersionless, and computed the Peierls constants for the $\mathbf{q} = 0$ eigenvectors only. Coupling to acoustic phonons, which is zero at $\mathbf{q} = 0$, is not considered. Within these approximations, symmetry arguments show that only the totally symmetric (A_g) phonons can be coupled to charge carriers. To evaluate the Peierls constants we have calculated the

TABLE 2 Low-energy A_g Phonons and Peierls Coupling of **H** Pentacene at $0\,K$

ω/cm^{-1}	$g_{\mathrm{VB}}/\mathrm{meV}$	$g_{\mathrm{CB}}/\mathrm{meV}$
27	8.2	7.2
61	7.1	4.9
70	0.5	3.1
96	3.7	5.5
132	1.1	1.0
148	6.9	0.0
156	3.8	5.9
162	1.5	1.6
203	7.2	5.5
206	2.8	3.0
238	3.7	1.5
241	1.0	1.5
259	5.4	2.8
261	3.8	2.4

hopping integrals, as detailed above, for the equilibrium and for geometries displaced along the QHLD eigenvectors. The $g(\boldsymbol{q}, j)$ are then obtained by numerical differentiation. In Table 2 we report the total Peierls coupling constants (sums of the modulations of the four hopping integrals defined in Fig. 3) for the **H** phase at $0\,K$.

Table 2 shows that several phonons are appreciably coupled to the charge carriers, and that some difference exists between the coupling in the VB and in the CB. The overall coupling strength, as measured by the lattice relaxation energy, $E_{LR} = \Sigma_j g_j^2/\omega_j$, is 35.3 and 26.9 meV for the VB and the CB band, respectively. The largest contribution to E_{LR} ($\sim 70\%$) comes from the two lowest frequencies modes, which are described as librations around the axes perpendicular to the long molecular axis, i.e., approximately parallel to the conducting ab plane (Figs. 1 and 3). Given the low frequency of these librations, they are likely to affect mobilities even at low temperatures. A more detailed analysis on the pentacene mobilities and their temperature dependence is in progress.

REFERENCES

[1] Dimitrakopoulos, C. D. & Mascaro, D. J. (2001). IBM *J. Res. & Dev.*, *45*, 11.

[2] Schön, J. H. (2001). *Phys. Stat. Sol.*, (b) *226*, 257 and refererences therein.

[3] See the Report of the Investigation Committee on the possibility of scientific misconduct in the work of H. Schön and coauthors, available at www.lucent.com.

[4] Campbell, R. B., Robertson J. M., & Trotter J. (1962). *Acta Cryst.*, *15*, 289.

[5] Holmes D., Kumaraswamy S., Matzger A. J., & Vollhardt, K. P. (1999). *Chem. Eur. J.*, *5*, 3399.

[6] Mattheus, C. C., Dros, A. B., Baas, J., Oostergetel, G. T., Meetsma, A., de Boer J. L., & Palstra T. M. (2003). *Synth. Metals*, 138, 475.

[7] Mattheus, C. C., de Wijs, G. A., de Groot, R. A., & Palstra, T. T. M. (2003). *J. Am. Chem. Soc.*, *125*, 6323. Northup J. E., Tiago, M. L., & Louie S. G. (2003). *Phys. Rev. B*, *66*, 121404(R).

[8] Venuti, E., Della Valle, R. G., Brillante, A., Masino, M., & Girlando, A. (2002). *J. Am. Chem. Soc.*, *124*, 2128.

[9] Masino, M., Girlando, A., Della Valle, R. G., Venuti, E., Farina, L., & Brillante, A. (2002). *Mat. Res. Soc. Symp. Proc.*, *725*, 149.

[10] Della Valle, R. G., Venuti, E., Brillante, A., & Girlando, A. (2003). *J. Chem. Phys.*, *118*, 807.

[11] Girlando, A., Masino, M., Visentini, G., Della Valle, R. G., Brillante, A., & Venuti, E. (2000). *Phys. Rev. B*, *62*, 14476.

[12] Della Valle, R. G. & Venuti, E. (1998). *Phys. Rev. B*, *58*, 206.

[13] Brillante, A., Della Valle, R. G., Farina, L., Girlando, A., Masino, M., & Venuti, E. (2002). *Chem. Phys. Lett.*, *357*, 32.

[14] Della Valle, R. G., Venuti, E., Farina, L., Brillante A., Masino M., & Girlando, A. *J. Phys. Chem. B*, 108, 1822.

[15] Farina, L., Syassen, K., Brillante, A., Della Valle, R. G., Venuti, E., & Karl, N. *High Press. Res.*, 23, 349. Farina, L., Brillante, A., Della Valle, R. G., Venuti E., Amboage, M., & Syassen, K. (2003). *Chem. Phys. Lett.*, 375, 490.

[16] Pope, M. & Swenberg, C. E. (1999). *Electronic Processes in Organic Crystals and Polymers*, Second Ed., Oxford University Press, New York.

[17] Cheng, Y. C., Silbey R. J., da Silva Filho, D. A., Calbert, J. P., Cornil, J., & Brédas, J. L. (2003). *J. Chem. Phys.*, *118*, 3764, and references therein.

[18] Zerner, M. C., Loew, G. H., Kirchner, R. F., & Mueller-Westerhoff, U. T. (1980). *J. Am. Chem. Soc.*, *102*, 589.

[19] Coropceanu, V., Malagoli, M., da Silva Filho, D. A., Gruhn, N. E., Bill, T. G., & Brédas, J. L. (2002). *Phys. Rev. Lett.*, *89*, 275503, 2002, and references therein.